Antibody-Mediated Inhibition of Ricin Toxin Retrograde Transport

Anastasiya Yermakova,[a,b] Tove Irene Klokk,[c] Richard Cole,[b,e] Kirsten Sandvig,[c,d] Nicholas J. Mantis[a,b]

Division of Infectious Disease, Wadsworth Center, New York State Department of Health, Albany, New York, USA[a]; Department of Biomedical Sciences, School of Public Health, University at Albany, Albany, New York, USA[b]; Department of Biochemistry, Centre for Cancer Biomedicine, Institute for Cancer Research, the Norwegian Radium Hospital, Oslo University Hospital, Montebello, Oslo, Norway[c]; Department of Biosciences, University of Oslo, Oslo, Norway[d]; Division of Translational Medicine, Wadsworth Center, New York State Department of Health, Albany, New York, USA[e]

ABSTRACT **Ricin is a member of the ubiquitous family of plant and bacterial AB toxins that gain entry into the cytosol of host cells through receptor-mediated endocytosis and retrograde traffic through the *trans*-Golgi network (TGN) and endoplasmic reticulum (ER). While a few ricin toxin-specific neutralizing monoclonal antibodies (MAbs) have been identified, the mechanisms by which these antibodies prevent toxin-induced cell death are largely unknown. Using immunofluorescence confocal microscopy and a TGN-specific sulfation assay, we demonstrate that 24B11, a MAb against ricin's binding subunit (RTB), associates with ricin in solution or when prebound to cell surfaces and then markedly enhances toxin uptake into host cells. Following endocytosis, however, toxin-antibody complexes failed to reach the TGN; instead, they were shunted to Rab7-positive late endosomes and LAMP-1-positive lysosomes. Monovalent 24B11 Fab fragments also interfered with toxin retrograde transport, indicating that neither cross-linking of membrane glycoproteins/glycolipids nor the recently identified intracellular Fc receptor is required to derail ricin en route to the TGN. Identification of the mechanism(s) by which antibodies like 24B11 neutralize ricin will advance our fundamental understanding of protein trafficking in mammalian cells and may lead to the discovery of new classes of toxin inhibitors and therapeutics for biodefense and emerging infectious diseases.**

IMPORTANCE **Ricin is the prototypic member of the AB family of medically important plant and bacterial toxins that includes cholera and Shiga toxins. Ricin is also a category B biothreat agent. Despite ongoing efforts to develop vaccines and antibody-based therapeutics against ricin, very little is known about the mechanisms by which antibodies neutralize this toxin. In general, it is thought that antibodies simply prevent toxins from attaching to cell surface receptors or promote their clearance through Fc receptor (FcR)-mediated uptake. In this report, however, we describe a neutralizing monoclonal antibody (MAb) against ricin's binding subunit (RTB) that not only associates with ricin after the toxin has bound to the cell's surface but actually enhances toxin uptake into host cells. Following endocytosis, the antibody-toxin complexes are then routed for degradation. The results of this study are important because they reveal a previously unappreciated role for B-subunit-specific antibodies in intracellular neutralization of ricin toxin.**

Received 21 November 2013 **Accepted** 6 March 2014 **Published** 8 April 2014

Citation Yermakova A, Klokk TI, Cole R, Sandvig K, Mantis NJ. 2014. Antibody-mediated inhibition of ricin toxin retrograde transport. mBio 5(2):e00995-13. doi:10.1128/mBio.00995-13.

Invited Editor Wayne Lencer, Children's Hospital Boston **Editor** R. John Collier, Harvard Medical School

Address correspondence to Nicholas J. Mantis, nmantis@wadsworth.org.

Ricin, a natural by-product of the castor bean plant (*Ricinus communis*), is a member of the AB superfamily of plant and bacterial protein toxins that exploit retrograde transport as a means to gain entry into the cytosol of host cells (1, 2). Cholera toxin (CT) and Shiga toxin (Stx) are also members of this family. Ricin's binding subunit (RTB) is a lectin that attaches to glycolipids and glycoproteins terminating in galactose and/or *N*-acetylgalactosamine (Gal/GalNAc) (3, 4). Following attachment to cell surfaces, RTB facilitates receptor-mediated endocytosis of ricin holotoxin via clathrin-dependent and -independent mechanisms (5). While the majority of ricin that is endocytosed is recycled back to the cell surface or shunted to lysosomes, a fraction of the internalized pool is trafficked retrograde to the *trans*-Golgi network (TGN) and the endoplasmic reticulum (ER) (5–7). Within the ER, the single disulfide bond that links RTA and RTB is reduced by protein disulfide isomerase (PDI), and RTA is then unfolded and retrotranslocated across the ER membrane into the cytoplasm (8). Once within the cytoplasm, RTA, an RNA *N*-glycosidase specific for the sarcin-ricin loop (SRL) of eukaryotic 28S rRNA, arrests protein synthesis and induces cell death through apoptosis (9).

There are ongoing initiatives by federal agencies to develop vaccines and antibody-based therapeutics against ricin, a category B biothreat agent for which there are currently no available countermeasures (10, 11). Considering its essential role in host cell binding and uptake, RTB is an obvious target for prophylactic and therapeutic antibodies. Indeed, the B subunit of CT is a component of one of the current oral *Vibrio cholerae* vaccines (12), and monoclonal antibodies (MAbs) against the B subunit of Stx are being pursued as possible therapeutics (13). In the case of ricin, however, only a few RTB-specific, toxin-neutralizing MAbs have been described to date, and very little is known about their mech-

anisms of action (2, 14–20). For example, we have produced and characterized dozens of RTB-specific MAbs, and only three, SylH3, JB4, and 24B11, were found to have toxin-neutralizing activity *in vitro* and were able to passively protect mice against a 10× 50% lethal dose (LD_{50}) ricin challenge (18–20). Similarly, Pringet and colleagues identified only two RTB-specific MAbs with toxin-neutralizing activity in their screen of ricin-specific B cell hybridomas (16). The vast majority of RTB-specific MAbs that have been described, including TFTB-1, bind ricin with high affinity but have no demonstrable toxin-neutralizing activity (18).

Recent work from our lab has revealed that two of the RTB-specific MAbs, SylH3 and 24B11, with virtually identical ricin-neutralizing activities likely function by different mechanisms, based on their ability to prevent toxin-receptor interactions. SylH3 IgG (and Fab fragments) inhibited ricin binding to plate-bound Gal/GalNAc glycoprotein residues, whereas 24B11 IgG (and Fab fragments) did not (18). Based on these and other data, we postulate that SylH3 and 24B11 represent two different types of RTB-specific, toxin-neutralizing MAbs. SylH3 and other MAbs described in the literature, including JB4, 75/3B12, and RB37, are type I MAbs in that they apparently neutralize ricin by steric hindrance (14, 16, 18–20). 24B11, a so-called "type II" MAb, neutralizes ricin by interfering with a step downstream of attachment, such as toxin endocytosis and/or intracellular trafficking.

In this report, we investigate the mechanism by which 24B11 neutralizes ricin toxin. We demonstrate that 24B11 is capable of associating with ricin after it has bound to cell surfaces and that ricin-24B11 complexes are readily endocytosed into Vero and HeLa cells. When in complex with 24B11, however, ricin's capacity to traffic retrograde to the TGN was virtually abolished. Ricin-24B11 complexes accumulated in late endosomes and eventually lysosomes, suggesting that the toxin-antibody complexes are likely subjected to proteolytic degradation. These findings reveal a previously unrecognized mechanism by which B-subunit-specific antibodies neutralize ricin and may have implications for understanding immunity to other members of the AB family of toxins.

RESULTS

24B11 neutralizes ricin when prebound to host cells. In a previous study, we demonstrated that 24B11 only partially inhibits the interaction of ricin with host cells, even though it is a highly potent toxin-neutralizing MAb (19). This observation led us to hypothesize that 24B11 neutralizes ricin by interfering with a step downstream of attachment (e.g., endocytosis or retrograde trafficking). If this hypothesis is correct, then we reasoned that 24B11 should be able to recognize ricin when bound to cell surfaces, whereas other RTB-specific MAbs, like SylH3 (which is proposed to neutralize ricin by blocking receptor interactions), and TFTB-1 (a nonneutralizing MAb that binds plate-bound ricin with high affinity) should not. Consistent with our hypothesis, 24B11 was able to recognize ricin that had been prebound to the surfaces of Vero and THP-1 cells (Fig. 1a; see Fig. S1 in the supplemental material). In contrast, neither SylH3 nor TFTB-1 was able to recognize ricin under those conditions. We also included R70 as a control in these assays. R70 (UNIVAX 70) is a toxin-neutralizing, murine IgG1 MAb directed against ricin's enzymatic subunit that does not affect ricin binding to host cells (21–23).

To determine whether the association of 24B11 with surface-bound ricin results in toxin neutralization, Vero and THP-1 cells were treated with ricin at 4°C, followed by 24B11 (or SylH3 or TFTB-1), and then shifted to 37°C to allow toxin internalization. For purposes of comparison, parallel toxin-neutralizing assays were performed in which MAbs were incubated with soluble ricin before being applied to Vero or THP-1 cells. We found that neither SylH3 nor TFTB-1 was capable of neutralizing prebound ricin, although SylH3 neutralized ricin when premixed with toxin before application to Vero (Fig. 1b) or THP-1 (see Fig. S2 in the supplemental material) cells. 24B11, on the other hand, neutralized ricin equally effectively, whether it was associated with ricin in solution or when prebound to cell surfaces (Fig. 1; see Fig. S2). These data are consistent with 24B11 neutralizing ricin at a step downstream of receptor binding.

24B11 interferes with retrograde trafficking of ricin to the TGN. We next used confocal laser scanning microscopy (CLSM) to examine whether 24B11 is internalized with ricin and, if so, whether it interferes with toxin intracellular trafficking. Vero cells grown on glass coverslips were incubated with fluorescein isothiocyanate (FITC)-labeled ricin for 30 min at 4°C and then treated with Alexa Fluor 633-labeled 24B11 (or TFTB-1) for an additional 30 min prior to being shifted to 37°C. At various time points thereafter (30 min, 90 min, and 4 h), cells were fixed and visualized by CLSM. In control cells (treated with ricin only) collected at 30 min, FITC-labeled ricin was localized within defined perinuclear vesicular compartments (Fig. 2A). After 90 min, ricin had coalesced around the nucleus with an appearance that was consistent with the toxin having undergone retrograde trafficking and vesicular fusion with the TGN (insets in Fig. 2A). Immunolabeling of cells taken at the 4-h time point confirmed that ricin colocalized with Golgin97, a marker of the TGN (Fig. 2B). As expected, uptake and retrograde trafficking of ricin were unaltered by the nonneutralizing MAb TFTB-1 (data not shown).

While 24B11 did not visibly affect endocytosis of ricin into Vero cells, the MAb inhibited trafficking of the toxin to the TGN. Specifically, at the 30-min time point, 24B11 and ricin colocalized within endocytic vesicles (Fig. 2A). The ricin-24B11-containing vesicles were similar in appearance to (but more numerous than) the ricin-containing vesicles observed in control cells. At 90 min, however, ricin-24B11-containing vesicles had not coalesced around the nucleus and did not stain positive for Golgin97 (Fig. 2B and C; see Fig. S3 in the supplemental material). Instead, ricin-24B11-containing vesicles remained distributed throughout the cytoplasm. The toxin-MAb-containing vesicles were also brighter and larger in diameter than ricin-positive vesicles in control cells at the same time point, indicating that they may be undergoing maturation to late endosomes (24). By 4 h, ricin-24B11 complexes were no longer detectable in vesicular compartments, although residual toxin-antibody complexes were evident at the cell periphery (Fig. 2A). These data demonstrate that 24B11 is internalized with ricin into host cells and then alters the toxin's capacity to traffic retrograde to the TGN.

To verify that the observed alterations in ricin retrograde trafficking in the presence of 24B11 were not an artifact of allowing 24B11 to associate with prebound ricin on cell surfaces, the microscopy studies were repeated, except that ricin and 24B11 were mixed in solution prior to being applied to Vero cells (see Fig. S4 in the supplemental material). A side-by-side comparison revealed that the intracellular patterns of ricin-24B11 staining were identical whether the toxin and MAb were mixed in solution and then applied to cells or whether 24B11 was allowed to associate with prebound ricin.

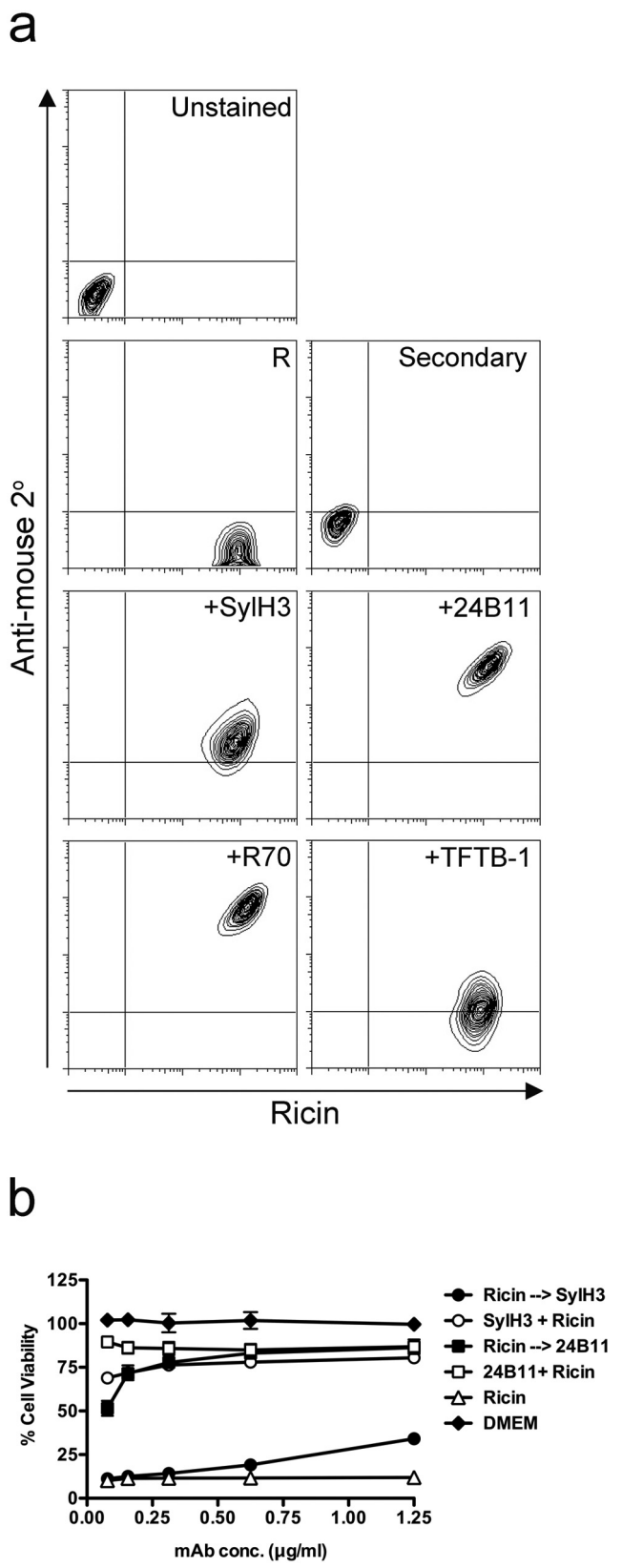

FIG 1 24B11 binds and neutralizes ricin when the toxin is prebound to cell surfaces. (a) Flow cytometric analysis of MAb recognition of ricin when the toxin is prebound to THP-1 cells. THP-1 cells were treated with ricin-FITC (R) for 30 min on ice prior to the addition of indicated antiricin MAbs (SylH3, *(Continued)*

We next exploited a TGN-specific sulfation assay to quantitate the retrograde trafficking of ricin-24B11 immune complexes in HeLa cells. The sulfation assay originally developed by Rapak and colleagues involves a recombinant variant of ricin toxin, known as RS1, in which RTA carries a C-terminal nanopeptide tyrosine sulfation motif that is modified upon entry into the TGN (25, 26). RS1 was mixed with 24B11, SylH3, or TFTB-1 and then applied to cells grown in the presence of $Na_2{}^{35}SO_4$. After 2 h, the total and RTA-specific levels of sulfation were determined (26). The total amount of RTA internalized into host cells was determined by Western blotting and densitometry.

Relative to the toxin-only-treated controls, 24B11 reduced TGN-specific sulfation of RTA by >80%, a result that is consistent with the CLSM studies (Fig. 3a). The observed reduction in RTA sulfation by 24B11 was not due to decreased levels of RS1 internalization, as 24B11 actually enhanced RS1 uptake into HeLa cells by almost 50% (Fig. 3b). SylH3 also reduced RTA sulfation by >80%, but this was due to the ability of the MAb to block toxin attachment to cell surfaces and prevent toxin internalization (Fig. 3a and b). Neither RTA sulfation nor RS1 internalization was significantly affected by the nonneutralizing MAb, TFTB-1.

We recently reported that 24B11 Fab fragments are as effective as the 24B11 IgG at neutralizing ricin *in vitro* and *in vivo* (19). To determine what effect Fab fragments have on retrograde transport of ricin, RS1 was mixed with 24B11, SylH3, or TFTB-1 Fab fragments and then applied to HeLa cells, as described above. In terms of RS1 sulfation, the Fab fragments performed almost identically to the corresponding full-length IgGs, indicating that neither cross-linking of membrane glycoproteins/glycolipids nor Fc receptor interactions are required to block toxin retrograde transport to the TGN (Fig. 3a and b). However, there were notable differences in how the Fabs influenced the fate of ricin within the cells. By microscopy, we observed that 24B11 Fab-toxin complexes resided in small cytoplasmic vesicles at early time points and then accumulated in the TGN at later time points (see Fig. S5a in the supplemental material), a pattern reminiscent of ricin itself more than ricin-24B11 IgG complexes. When 24B11 Fab-ricin complexes were treated with fluorophore-conjugated polyclonal anti-mouse H+L antibodies as a means to cross-link the Fab fragments, the 24B11 Fab-ricin complexes resembled 24B11-ricin complexes in that they accumulated in large perinuclear cytoplasmic vesicles within the cells and failed to merge with the TGN (see Fig. S5b). Thus, while both 24B11 Fabs and full-length IgG are sufficient to block retrograde transport of ricin, as determined by the RS1 sulfation assay, they may do so by different mechanisms based on their ability to promote toxin cross-linking.

24B11-ricin complexes accumulate in late endosomes and lysosomes. To define the fate of 24B11-ricin complexes following

Figure Legend Continued

24B11, R70, and TFTB-1). The cells were then washed and probed with PerCP-labeled anti-mouse $F(ab')_2$ before being subjected to flow cytometry. Scales on the *x* axis (FITC channel) and *y* axis (PerCP channel) represent $\log_{10}$ mean fluorescence intensity (MFI). (b) 24B11 and SylH3 were assessed for toxin-neutralizing activity when mixed with ricin in solution (open circles or open squares) or when ricin was prebound to Vero cell surfaces (solid circles or solid squares), as described previously (18, 48). Cell death was assessed using CellTiter-GLO (Promega, Madison, WI). Data are representative of 3 independent experiments. Percent viability was normalized to the values obtained from cells treated with medium only.

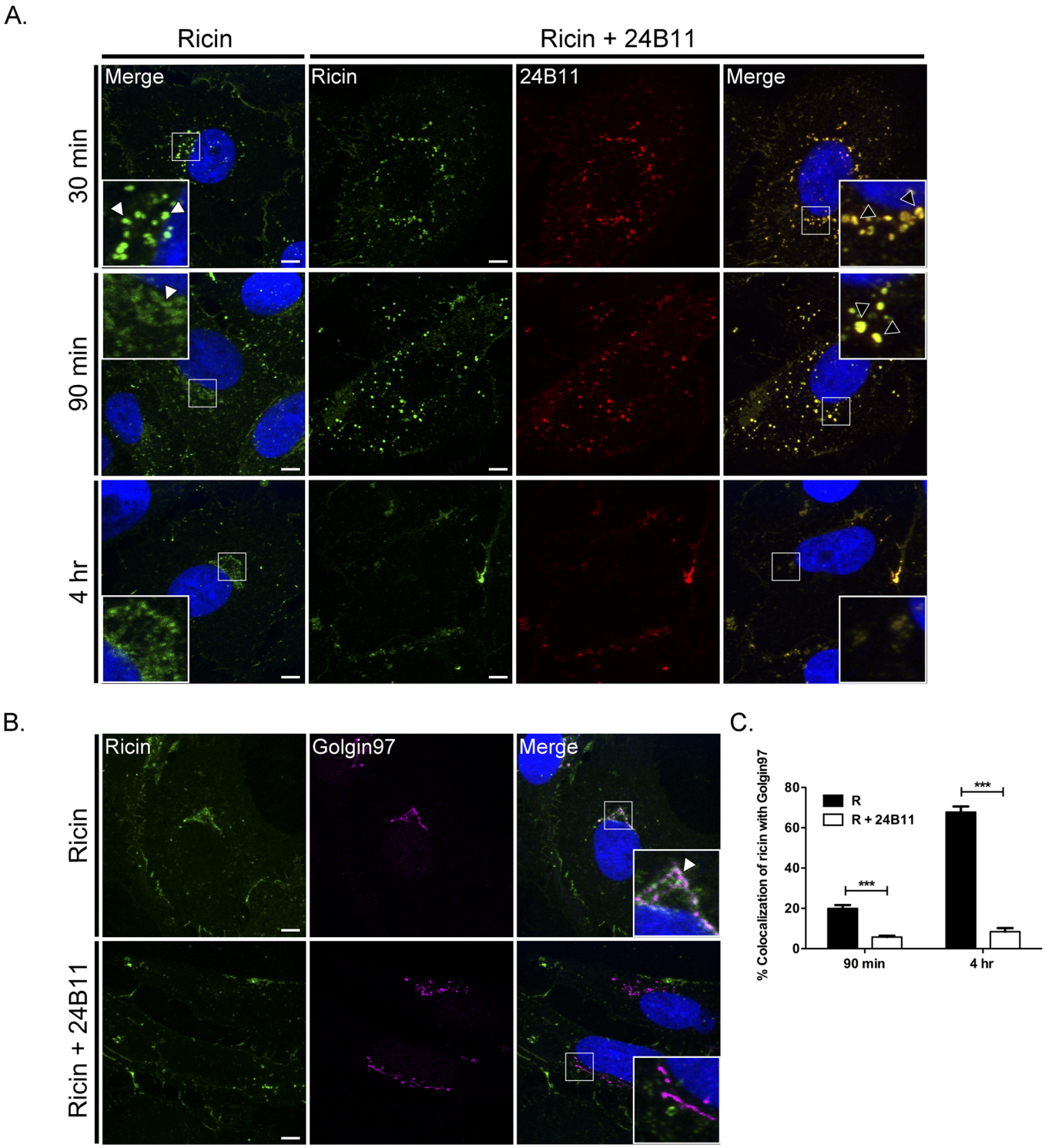

FIG 2 24B11 is internalized with ricin and alters the toxin's intracellular trafficking. (A) Vero cells, grown on glass coverslips, were cooled to 4°C and incubated for 30 min with ricin-FITC. The cells were then washed, treated (or not) with Alexa Fluor 633-labeled 24B11 for an additional 30 min at 4°C, and then shifted to 37°C. At the indicated time points (30 min, 90 min, and 4 h) the cells were fixed and imaged by confocal microscopy. Insets in the right- and left-hand columns highlight the subcellular localization of ricin (white arrowheads) and ricin-24B11 complexes (black arrowheads). Images are representative of at least four independent experiments. Scale bar, 5 μm. (B and C) Cells treated with ricin or ricin-24B11 were collected at 90 min or 4 h (as described above) and then immunolabeled with Golgin97 to localize the *trans*-Golgi network (TGN). (B) Representative images taken at the 4-h time point indicating the visual colocalization of ricin with Golgin97 in the absence (top panels) but not in the presence of 24B11 (bottom panels). The arrowhead (inset, top right panel) indicates colocalization between ricin (green) and Golgin97 (magenta) staining. Each image is a maximum-intensity projection of 20 to 30 z-stacks (0.13-μm thickness). Scale bar, 5 μm. (C) The frequency of ricin colocalization with Golgin97 at the indicated time points was quantitated with ImageJ, as described in Materials and Methods. At least 30 cells were analyzed from each time point. ***, $P < 0.001$.

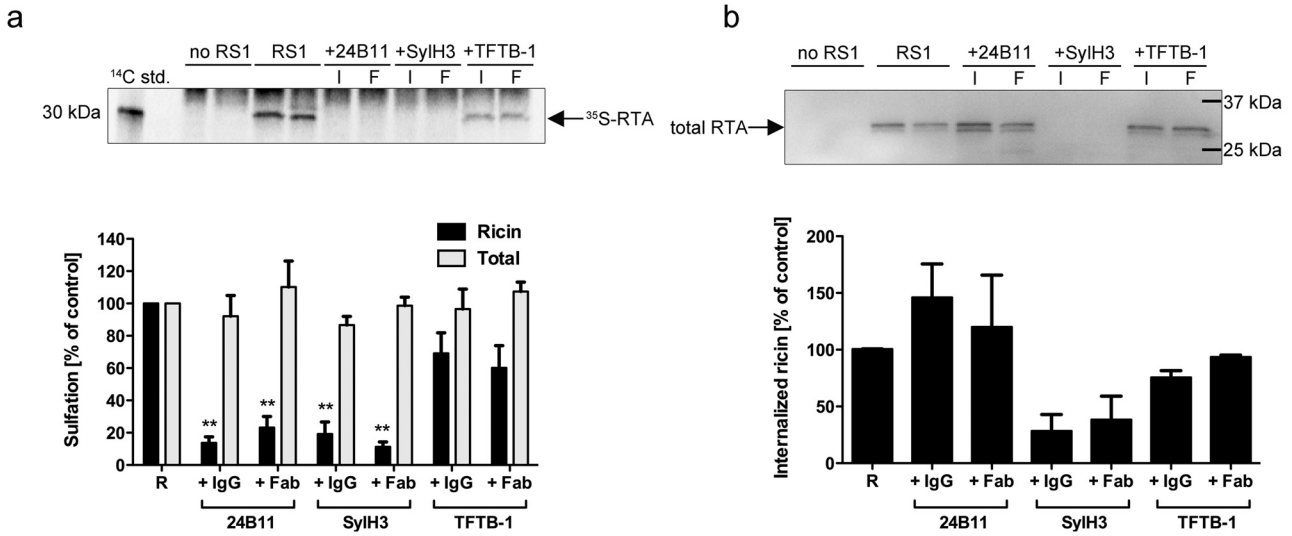

FIG 3 24B11 inhibits retrograde transport of ricin to the TGN. Cells were incubated with $Na_2{}^{35}SO_4$ prior to the addition of RS1 in the absence or presence of the indicated MAbs (I) or Fabs (F). Two hours later, the cells were washed with buffer containing lactose to remove any residual surface-bound ricin and then lysed. Precipitated proteins from lysates were subjected to SDS-PAGE and transferred to a PVDF membrane. (a) Specific RTA sulfation was measured by autoradiography (top panel) and quantitated by densitometry (bottom panel). Total sulfation was determined by precipitation of the remaining lysate. std., standard. Each bar (mean with standard deviation [SD]) represents the average of three independent experiments. The asterisks ($P < 0.01$) represent significance between the percent sulfated ricin control and sulfated ricin plus MAb, as determined using an unpaired *t* test with a 95% confidence interval. (b) After the sulfation assay, the membrane was subjected to Western blot analysis with an anti-RTA antibody (top panel) and then quantitated by densitometry (bottom panel).

endocytosis, toxin- and toxin-MAb-treated Vero cells were stained for EEA-1, a marker of early endosomes (EEs), or Rab11, a marker of recycling endosomes (REs). In the toxin-only-treated cells, ricin colocalized with EEA-1 at 30 min but not at 90 min (see Fig. S6 in the supplemental material). Similarly, 24B11-ricin complexes colocalized with EEA-1-positive vesicles at 30 min but not at 90 min or later time points, suggesting that 24B11 does not delay ricin egress from the EEs or divert the toxin from its normal trafficking pathway at this step. Likewise, ricin and 24B11-ricin complexes colocalized with the EE protein Rab5 at 30 min but not at 90 min (data not shown). 24B11 did not, however, promote prolonged accumulation of ricin in REs, as neither ricin nor 24B11-ricin complexes colocalized with Rab11 at any of the time points examined (see Fig. S7 in the supplemental material).

Based on these observations, we postulated that ricin-24B11 complexes are trafficked to lysosomes for degradation. To test this hypothesis, toxin- and toxin-MAb-treated Vero cells were stained for Rab7, a marker of late endosomes (LEs) (Fig. 4; see Fig. S8 in the supplemental material). We expected that a large amount of ricin would by default colocalize with Rab7, considering the majority (>90%) of toxin is known to be degraded following endocytosis (7). Indeed, at the 30-min time point, ~70% of ricin-containing vesicles were positive for Rab7 (Fig. 4B; see Fig. S8). At 90 min, <40% of the ricin-containing vesicles were Rab7 positive, indicative of the fact that most of the residual toxin had now reached the TGN or the lysosomes (Fig. 4A and B). Examination of cells treated with 24B11-toxin complexes revealed that ricin localized within Rab7-positive vesicles at both 30- and 90-min time points at significantly greater levels than was observed in ricin-only treated cells (Fig. 4A and B; see Fig. S8). The trafficking of 24B11 to Rab7-positive vesicles was not Fc dependent, as 24B11 $F(ab')_2$ fragments also promoted the accumulation of ricin within these vesicles by 90 min (see Fig. S9 in the supplemental material).

Because 24B11-ricin complexes were concentrated within vesicles positive for Rab7 at 30 and 90 min, but were not detectable in these structures at the 4-h time point, we postulated that the complexes were likely being degraded via lysosomes. To test this experimentally, Vero cells were incubated in the presence of 10 mM NH_4Cl, an inhibitor of endosome-lysosome acidification, prior to being treated with 24B11-ricin complexes. In the absence of NH_4Cl, ricin-24B11 complexes were not detectable at 4.5 h, whereas in the presence of NH_4Cl, ricin-24B11 complexes had accumulated in large cytoplasmic vesicles that were positive for Rab7 and the lysosomal marker Lamp-1 (Fig. 5A and B; see Fig. S10 in the supplemental material). Quantitative analysis confirmed that in NH_4Cl-treated cells at 4.5 h, ricin-24B11 complexes were more frequently associated with Rab7 and Lamp-1 vesicles than ricin from control cells (Fig. 5c; see Fig. S10). These data are consistent with 24B11 shunting ricin to lysosomes for degradation.

DISCUSSION

Neutralizing antibodies directed against the binding subunits of AB toxins like ricin, CT, and Stx are generally assumed to simply interfere with toxin attachment to host cell receptors. 24B11 is unique in this respect because it neutralizes ricin without significantly affecting toxin-receptor interactions (18, 20). This unusual property led us to propose that 24B11 neutralizes ricin by interfering with toxin internalization and/or intracellular trafficking. In this study, we demonstrated that 24B11 not only recognizes receptor-bound ricin but also actually enhances toxin uptake into host cells. However, following endocytosis, ricin-24B11 complexes failed to traffic retrograde to the TGN. Instead, ricin-24B11 complexes were shunted to Rab7-positive vesicles and LEs, likely resulting in lysosome-mediated proteolytic degradation. While the precise mechanism by which 24B11 interferes with ricin's nor-

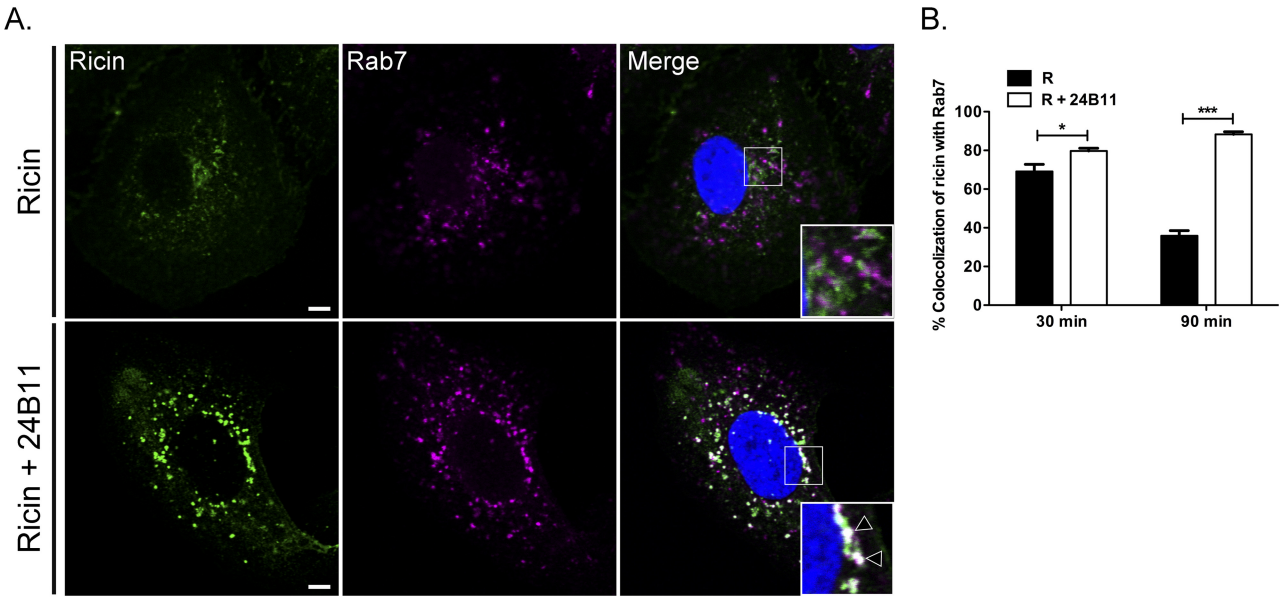

FIG 4 24B11-ricin toxin complexes accumulate in late endosomes. Vero cells treated at 4°C with ricin-FITC (A, top panels) or ricin-FITC and 24B11 (A, bottom panels), as described in the Materials and Methods, were shifted to 37°C for 30 min (see >Fig. S8 in the supplemental material) or 90 min before being fixed and stained for Rab7 (magenta). Insets (right column) indicate minimal visual colocalization between ricin and Rab7 in the absence of 24B11 but notable overlap in the presence of 24B11 (arrowheads). Scale bars, 5 μm. Images are representative of at least six independent experiments. (B) The frequency of ricin colocalization with Rab7 at the 30- and 90-min time points was quantitated with ImageJ, as described in Materials and Methods. Each bar represents the average of 12 to 15 cells (with standard error of the mean [SEM]) of 6 individual experiments. *, $P < 0.05$; ***, $P < 0.001$ (determined using an unpaired t test with a 95% confidence interval).

mal retrograde transport pathway remains to be elucidated, the fact that Fab and F(ab′)$_2$ fragments interfered with toxin transport to the TGN (described below) rules out a role for Fc receptors, including TRIM21, in 24B11-mediated neutralization of ricin (19, 27).

The structure of RTB provides few obvious clues as to how 24B11 interferes with retrograde transport of ricin. RTB consists of two globular domains with identical folding topologies and has been compared to an elongated "dumbbell" (28). Each of the two domains (1 and 2) is comprised of three homologous subdomains (α, β, and γ) that probably arose by gene duplication from a primordial carbohydrate recognition domain (CRD) (3). Only the external subdomains, 1α and 2γ, which are separated by ~70 Å, retain galactoside recognition activity (3, 29). The two CRDs bind galactosides in a noncooperative manner, although a recent study has suggested otherwise (30–33). RTB also has two N-linked high-mannose side chains that have been postulated to interact with mannose-binding protein(s) during ricin toxin intracellular transport and/or influence intracellular stability of RTB (26, 34–37). 24B11 is proposed to recognize an epitope encompassing a small solvent-exposed loop situated between (and in close proximity to) the CRD and the N-linked oligosaccharide side chain on RTB's domain 1 (15, 20).

Ricin uptake and intracellular transport in mammalian cells have been studied for decades, and we can envision several possible means by which 24B11 might interrupt ricin trafficking. It is now well established, for example, that altering the valence and/or size of ricin alters the efficiency of retrograde transport. We (K.S.) originally demonstrated this by covalently coupling ricin to colloidal gold or polyvalent horseradish peroxidase, which resulted in impaired trafficking of ricin to the TGN (38). More recently, we (K.S.) demonstrated that coupling ricin to quantum dot bioconjugates (26 nm in diameter) did not affect ricin internalization but did inhibit retrograde transport (39). Thus, it is possible that 24B11 promotes cross-linking of ricin on the plasma membrane and that 24B11-toxin complexes are simply routed, by default, to LEs and lysosomes.

While cross-linking of ricin on the plasma membrane is an appealing model that is well supported by a number of lines of evidence, it does not explain why monovalent 24B11 Fab fragments are as effective as full-length IgG at neutralizing ricin and blocking sulfation of recombinant RS1. Perhaps Fab fragments interfere with ricin retrograde transport by a different mechanism than full-length IgG? This possibility is supported by the observation that 24B11 Fab-toxin complexes tended to reside in small cytoplasmic vesicles at early time points following uptake and then eventually accumulated in the TGN, whereas 24B11 IgG-toxin complexes clustered in large vesicles and never reached the TGN at detectable levels. How then can we account for the absence of RS1 sulfation? In fact, very little is known about the actual mechanism of RTA sulfation in the TGN (25, 40), so the possibility that 24B11 Fab fragments interfere directly with the sulfation event through steric hindrance (or another mechanism) cannot be excluded.

Alternatively, perhaps 24B11 prevents ricin from interacting with one or more host proteins required for the early stages of retrograde transport. While this seems like a plausible model, considering that a number of host factors involved in transport of ricin to the TGN have been described, no one specific protein or lipid has been shown to specifically associate with RTB (see reviews in references 6 and 41). Another shortcoming of this model is that ricin is known to be an "opportunist" in the sense that,

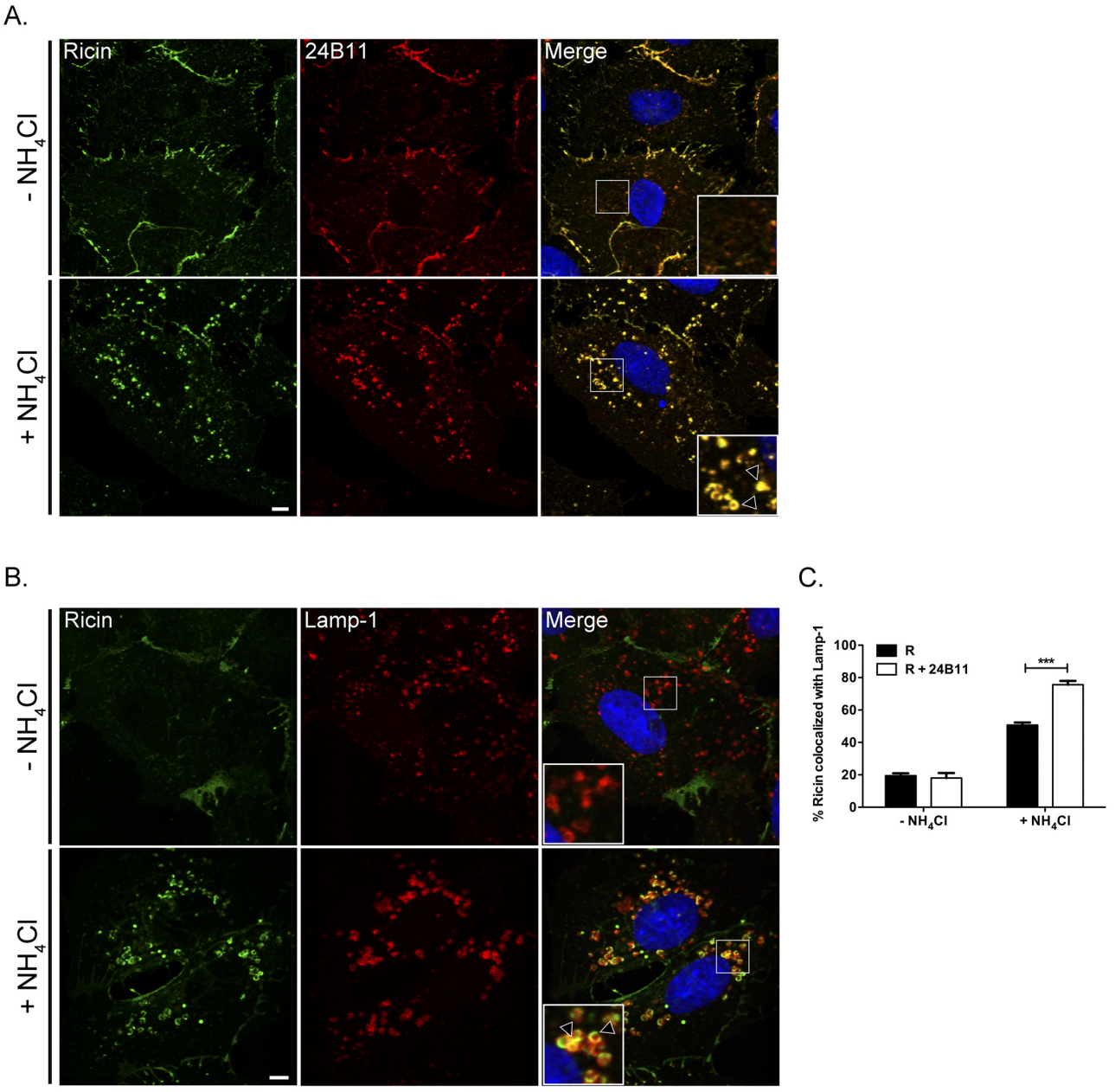

FIG 5 Ricin-24B11 complexes traffic to lysosomes. Vero cells were treated at 4°C with 24B11 and ricin-FITC, in the absence or presence of NH_4Cl to prevent lysosome acidification, and then shifted to 37°C for 4.5 h. Vero cells were then fixed and stained with DyLight 650-labeled goat anti-mouse IgG Fabs (A) to detect 24B11 (not shown) or Alexa Fluor 647-labeled Lamp-1 antibodies (B). NH_4Cl treatment resulted in the accumulation of ricin-24B11-containing vesicles that were positive for Lamp-1 (arrowheads within insets, bottom right panels). Scale bar, 5 μm. (C) Frequency of ricin (in the absence or presence of 24B11) colocalization with Lamp-1 in cells treated or not with NH_4Cl. Each bar represents the average of 30 cells (with SEM) per time point. ***, $P < 0.001$ (as determined using an unpaired *t* test with a 95% confidence interval).

unlike Stx, it does not rely on one specific intracellular pathway by which to gain entry into the TGN. Rather, ricin appears to exploit multiple pathways to the TGN (42). It should be noted at this point that a small molecule known as Retro-2 was recently identified as being a potent inhibitor of endosome to TGN transport of Stx and ricin and in this sense is a "phenocopy" of 24B11 (42, 43). Retro-2, however, exerts its effect by targeting a host protein and not the toxin *per se*. Whether there is a connection between the mode of action of 24B11 and Retro-2 remains to be determined.

While there is mounting evidence to suggest that antibodies against the A subunits of ricin and Stx neutralize intracellularly (23, 44–46), our present study is the first (to our knowledge) to demonstrate that an antibody to ricin's or Stx's binding subunit interferes with a step other than blocking receptor attachment. It will be interesting to determine whether 24B11 is an anomaly or whether others have identified so-called "type II" MAbs like 24B11 but simply not investigated the possibility that they function in an atypical manner (14, 16). We are ultimately interested in

TABLE 1 Sources of primary and secondary antibodies used in this study

Target	Dilution	Source species	Conjugate	Vendor[a]
Rab7	1:30	Rabbit	UL	Cell Signaling Technology
Rab11	1:50	Rabbit	UL	Cell Signaling Technology
EEA1	1:100	Rabbit	UL	Abcam
Golgin97	1:40	Rabbit	UL	Abcam
Lamp-1	1:20	Mouse	Alexa Fluor 647	BioLegend
Anti-mouse IgG (H+L)	1:50	Goat	PerCP	Jackson ImmunoResearch
	1:300	Goat	DyLight 650	Leinco Technologies
	1:200	Rabbit	DyLight 549	Jackson ImmunoResearch
Anti-rabbit IgG (H+L)	1:200	Goat	DyLight 649	Jackson ImmunoResearch
	1:200	Goat	Alexa Fluor 633	Life Technologies
Anti-mouse IgG (H+L)	1:200	Goat	Alexa Fluor 546	Life Technologies

[a] Cell Signaling Technology, Beverly, MA; Abcam, Cambridge, MA; BioLegend, San Diego, CA; Jackson ImmunoResearch, Bar Harbor, ME; Leinco Technologies, Fenton, MO; Life Technologies, Carlsbad, CA.

defining the relative contributions of type I and type II antibodies, within the context of a polyclonal antibody response, in eliciting protective immunity and whether these different activities can be leveraged with respect to vaccine and therapeutic design and development.

MATERIALS AND METHODS

Chemicals, biological reagents, supplies, and cell lines. Ricin toxin (*Ricinus communis* agglutinin II) and ricin-FITC were purchased from Vector Laboratories (Burlingame, CA). Ricin was dialyzed against phosphate-buffered saline (PBS) at 4°C in 10,000-molecular-weight-cutoff Slide-A-Lyzer dialysis cassettes (Thermo Scientific, Rockford, IL) prior to use in cell-based studies. Tween 20, Triton X-100, Parafilm, and Hoechst 33342 were purchased from Sigma-Aldrich (St. Louis, MO). ProLong Gold with 4′,6-diamidino-2-phenylindole (DAPI), Image-iT Fx signal enhancer, and the Alexa Fluor 633 protein labeling kit were purchased from Life Technologies (Carlsbad, CA). The commercial secondary and primary Abs used in this study are described in Table 1. Glass coverslips (22- by 22-mm square, 1.5 mm) were purchased from Corning-Fischer Scientific (Suwanee, GA). Tissue culture-treated dishes (35 mm by 15 mm) were purchased from Celltreat Scientific Products (Shirley, MA). Cytofix/Cytoperm fixation/permeabilization solution was purchased from BD Biosciences (San Jose, CA). White 96-well plates were obtained from Corning Life Sciences (Corning, NY). GlutaMax, fetal calf serum, and goat serum were purchased from Gibco-Invitrogen (Carlsbad, CA). Vero cells, THP-1 cells, and cells of the murine myeloma cell line P3X63.Ag8.653 were purchased from the American Type Culture Collection (Manassas, VA). Unless otherwise noted, all cell lines were maintained in a humidified incubator at 37°C with a 5% CO_2 atmosphere.

Ricin MAbs. Murine MAbs 24B11, SylH3, TFTB-1, and R70 have been described previously (18, 22). TFTB-1 is an RTB-specific, nonneutralizing MAb that has high affinity (equilibrium dissociation constant [K_D], 5.63×10^{-9}) for plate-bound ricin (18). R70 (also known as UNIVAX-70) is an RTA-specific neutralizing MAb described by Lemley and colleagues (21). MAb purification was done using ion-exchange (IEX) and protein G chromatography under endotoxin-free conditions by the Wadsworth Center's Protein Expression core facility. Fab and $F(ab')_2$ fragments were produced using the mouse IgG1 Fab and $F(ab')_2$ preparation kit (Pierce, ThermoScientific, Rockford, IL) (19).

Cytotoxicity, apoptosis, and antibody binding assays. Ricin-induced apoptosis of THP-1 cells was assessed using the Annexin V-FITC apoptosis detection kit II (BD Pharmingen). THP-1 cells (5×10^5) were incubated with ricin (2.5 μg/ml) in the presence or absence of anti-RTB MAbs (40 μg/ml) for 5 h in 96-well Microtest U-bottom tissue culture treated plates (BD Biosciences, San Jose, CA) at 37°C. The cells were then collected by centrifugation, washed in sorting buffer (1 mM EDTA, 25 mM HEPES, pH 7.0, 1% fetal bovine serum [FBS] in Ca^+/Mg^+-free PBS), and stained with Annexin V-FITC. To determine if the MAbs were capable of neutralizing ricin when prebound to cells, THP-1 cells (5×10^5) were incubated with ricin for 30 min at 4°C, washed, and then treated with anti-RTB MAbs for an additional 30 min at 4°C. The cells were transferred to 37°C and incubated for 5 h before being stained with Annexin V-FITC, as described above. A minimum of 10,000 cells were analyzed per sample using a FACSCalibur fluorescence-activated cell sorter (BD Biosciences).

To quantitate the ability of MAbs to recognized ricin bound on cell surfaces, THP-1 cells (1×10^6) were incubated for 20 min at 4°C and then treated with ricin-FITC (3 μg/ml) for an additional 30 min at 4°C. The cells were then washed to remove unbound toxin and probed with antiricin MAbs (20 μg/ml). The cells were incubated for 30 min on ice, washed, and then labeled with $F(ab')_2$-peridinin chlorophyll protein (PerCP) (Jackson ImmunoResearch) for 30 min before being fixed in 4% paraformaldehyde (PFA) in PHEM buffer [60 mM piperazine-*N*,*N*′-bis(2-ethanesulfonic acid) (PIPES), 25 mM HEPES, 10 mM EGTA, 2 mM $MgCl_2$, pH 6.9] for 15 min. Cells were diluted into Ca^+/Mg^+-free Hanks' balanced salt solution (HBSS) and analyzed by flow cytometry using a FACSCalibur. A minimum of 10,000 cells were analyzed per sample.

Ricin-specific sulfation assays. Ricin-sulf-1 (RS1), which is ricin with a modified ricin A-subunit containing a tyrosine sulfation site, was produced and purified as described previously (25). HeLa and Vero cells were washed with sulfate-free HEPES-buffered medium supplemented with 2 mM L-glutamine, followed by incubation with 0.2 mCi/ml $Na_2{}^{35}SO_4$ (Hartmann Analytic, Braunschweig, Germany) in sulfate-free HEPES-buffered medium for 2.5 h at 37°C. RS1 was preincubated with the indicated anti-RTB MAbs for 30 min at room temperature, before the mixture was applied to cells and incubated for 2 h at 37°C. The cells were then washed (2×5 min) with 0.1 M lactose in HEPES-buffered medium and once in cold PBS on ice before the addition of 400-μl lysis buffer (0.1 M NaCl, 10 mM Na_2HPO_4, 1 mM EDTA, 1% Triton X-100, 60 mM octylglycopyranoside) supplemented with complete protease inhibitors (Roche Diagnostics, Mannheim, Germany). The lysate was cleared by centrifugation (8,000 rpm, 10 min, 4°C), and 300 μl of the supernatant was mixed with 1 ml 5% trichloroacetic acid (TCA) followed by centrifugation at 14,000 rpm (10 min, 4°C). The resulting pellet was washed once in ice-cold PBS, dissolved in 2× sample buffer, and subjected to SDS-PAGE under reducing conditions, followed by blotting onto a polyvinylidene difluoride (PVDF) membrane (Immobilon-P; Millipore, Billerica, MA). The bands were detected by autoradiography using a PharosFX scanner and quantified using Quantity One 1-D Analysis software (BioRad Laboratories, Inc., Hercules, CA). The total amount of sulfated proteins was determined by TCA precipitation of the remaining lysates.

For the purpose of quantification of ricin internalization after the sulfation assay, the resulting PVDF membrane was rewet in PBS-T (PBS with 0.01% Tween 20) and then probed overnight at 4°C with polyclonal anti-RTA antibody (Abcam, Cambridge, MA) in 5% BSA in PBS-T. The membrane was then repeatedly washed with PBS-T and probed with

(HRP)-conjugated secondary antibody (Jackson Immunoresearch) that had been diluted in 1% BSA in PBS-T. The membranes were developed using the ECL enhanced chemiluminescence Western blotting detection reagent (GE Healthcare, Buckinghamshire, United Kingdom) and quantified using Quantity One 1-D Analysis software (Bio-Rad, Oslo, Norway).

Analysis of ricin endocytosis by confocal fluorescence microscopy. Vero or HeLa cells were seeded onto sterile glass coverslips in 6-well tissue culture plates at a density of 1.5×10^5 cells/well and incubated for 24 h to achieve 50 to 70% confluence. Cells were cooled to 4°C for 30 min before the coverslips were inverted onto a droplet of ricin-FITC (10 μg/coverslip) situated on Parafilm and then incubated in a humidified chamber for an additional 30 min. The coverslips were rinsed with 10% FBS in DMEM (at 4°C) and then inverted onto a droplet of Alexa Fluor 633-labeled 24B11 (6 μg/ sample) or control MAb. The coverslips were incubated at 4°C for 30 min before being transferred to sterile tissue culture dishes (35 mm by 15 mm) containing prewarmed medium. The cells were incubated at 37°C for specific time points (30 to 320 min) before being rinsed with PHEM buffer, fixed with 4% PFA (in PHEM), and then permeabilized with 0.5% Triton X-100 (in PHEM) for 1 min. Cells were washed (4× 5 min) in PHEM and blocked first with Image-iT Fx signal enhancer for 30 min and then PBS-Tween (0.5%) supplemented with Superblock solution (5% normal goat serum and 5% BSA) for staining with anti-EEA1 or anti-Golgin97 antibodies, or Superblock Plus solution (5% normal goat serum, 5% BSA, and 5% Carnation instant nonfat dry milk) for anti-Rab7 and anti-Rab11 staining. Incubations with Rab7 and Rab11 Abs were done overnight at room temperature, while EEA1 and Golgin97 antibody incubations were done for 1 h at 37°C. Anti-Lamp-1 antibody staining was performed as per the instructions in the BD Cytofix/Cytoperm fixation/permeabilization solution kit. The primary and secondary antibodies used in this study are listed in Table 1.

Following immunolabeling, cells were washed with PHEM buffer, stained with Hoechst (1 μg/ml) for 5 min, washed again, and then mounted onto glass microscope slides with ProLong Gold. Cells were imaged using a Leica TCS SP5 AOBS (acousto-optical beam splitter) confocal microscope with multiphoton laser and a 63× objective (1.4 NA) in a sequential manner (Leica Microsystems, Inc., Buffalo Grove, IL). In general, image slices were collected midway through the volume of the cells where the vesicles and TGN were located. z-stack steps (20 to 35 z-stacks) were 0.13 μm. The frequency of ricin-FITC colocalization with Rab7, EEA1, Lamp-1, or Golgin97 was determined using Manders' coefficients within the Just Another Colocalization Plugin (JACoP) for ImageJ (47). Ricin-FITC-positive vesicles were selected using ImageJ's freehand selection option, and the percentage of colocalization was determined by measuring the selected fraction of ricin-FITC that overlaps with Rab7, EEA1, or Lamp-1-positive vesicles or Golgin97. Cell slices were used for quantitation of markers Rab7, EEA1, and Lamp-1, and a maximum projection of z-stacks was used for the Golgin97 marker.

Statistical analysis and software. Statistical analysis was carried out with GraphPad Prism 5 (GraphPad Software, San Diego, CA). Microscopy image processing and analysis were done using ImageJ 1.46j (public domain) and Adobe Photoshop CS4 (Adobe Systems, Inc., San Jose, CA).

SUPPLEMENTAL MATERIAL

Supplemental material for this article may be found at http://mbio.asm.org/lookup/suppl/doi:10.1128/mBio.00995-13/-/DCSupplemental.

Figure S1, TIF file, 2.4 MB.
Figure S2, TIF file, 1.8 MB.
Figure S3, TIF file, 2.1 MB.
Figure S4, TIF file, 2.5 MB.
Figure S5, TIF file, 2.8 MB.
Figure S6, TIF file, 2.6 MB.
Figure S7, TIF file, 2.6 MB.
Figure S8, TIF file, 2.7 MB.
Figure S9, TIF file, 2.6 MB.
Figure S10, TIF file, 2.8 MB.

ACKNOWLEDGMENTS

We acknowledge Renjie Song of the Wadsworth Center's Immunology Core for assistance with the flow cytometry analysis and Karen Chave of the Northeast Biodefense Center's Protein Purification Core at the Wadsworth Center for assistance with antibody purification. We acknowledge of the Wadsworth Center's Advance Light Microscopy and Image Analysis Core for assistance with the imaging and image analysis. We thank Jennifer Yates and Eric Smith for technical assistance and Joanne O'Hara, Kathleen McDonough, and Jim Drake (AMC) for critical feedback and insight.

This work was supported by grant AI097688 (principal investigator, N. J. Mantis) from the National Institutes of Health. A.Y. was supported in part by a predoctoral fellowship from the Wadsworth Center's Biodefense and Emerging Infectious Diseases Program (T32AI055429; principal investigator, K. A. McDonough). T.I.K. and K.S. were supported by grants from the South-Eastern Norway Regional Health Authority.

REFERENCES

1. **Johannes L, Römer W.** 2010. Shiga toxins—from cell biology to biomedical applications. Nat. Rev. Microbiol. **8:**105–116. http://dx.doi.org/10.1038/nrmicro2279.
2. **O'Hara JM, Yermakova A, Mantis NJ.** 2012. Immunity to ricin: fundamental insights into toxin-antibody interactions. Curr. Top. Microbiol. Immunol. **357:**209–241. http://dx.doi.org/10.1007/82_2011_193.
3. **Rutenber E, Ready M, Robertus JD.** 1987. Structure and evolution of ricin B chain. Nature **326:**624–626. http://dx.doi.org/10.1038/326624a0.
4. **Sandvig K, Olsnes S, Pihl A.** 1976. Kinetics of binding of the toxic lectins abrin and ricin to surface receptors of human cells. J. Biol. Chem. **251:** 3977–3984.
5. **Sandvig K, Skotland T, van Deurs B, Klokk TI.** 2013. Retrograde transport of protein toxins through the Golgi apparatus. Histochem. Cell Biol. **140:**317–326. http://dx.doi.org/10.1007/s00418-013-1111-z.
6. **Johannes L, Popoff V.** 2008. Tracing the retrograde route in protein trafficking. Cell **135:**1175–1187. http://dx.doi.org/10.1016/j.cell.2008.12.009.
7. **van Deurs B, Sandvig K, Petersen OW, Olsnes S, Simons K, Griffiths G.** 1988. Estimation of the amount of internalized ricin that reaches the trans-Golgi network. J. Cell Biol. **106:**253–267. http://dx.doi.org/10.1083/jcb.106.2.253.
8. **Spooner RA, Watson PD, Marsden CJ, Smith DC, Moore KA, Cook JP, Lord JM, Roberts LM.** 2004. Protein disulphide-isomerase reduces ricin to its A and B chains in the endoplasmic reticulum. Biochem. J. **383:** 285–293. http://dx.doi.org/10.1042/BJ20040742.
9. **Jandhyala DM, Thorpe CM, Magun B.** 2012. Ricin and Shiga toxins: effects on host cell signal transduction. Curr. Top. Microbiol. Immunol. **357:**41–65. http://dx.doi.org/10.1007/82_2011_181.
10. **Reisler RB, Smith LA.** 2012. The need for continued development of ricin countermeasures. Adv. Prev. Med. 2012:149737. http://dx.doi.org/10.1155/2012/149737.
11. **Wolfe DN, Florence W, Bryant P.** 2013. Current biodefense vaccine programs and challenges. Hum. Vaccin. Immunother. **9:**1591–1597. http://dx.doi.org/10.4161/hv.24063.
12. **Pasetti MF, Levine MM.** 2012. Insights from natural infection-derived immunity to cholera instruct vaccine efforts. Clin. Vaccine Immunol. **19:** 1707–1711. http://dx.doi.org/10.1128/CVI.00543-12.
13. **Tzipori S, Sheoran A, Akiyoshi D, Donohue-Rolfe A, Trachtman H.** 2004. Antibody therapy in the management of Shiga toxin-induced hemolytic uremic syndrome. Clin. Microbiol. Rev. **17:**926–941. http://dx.doi.org/10.1128/CMR.17.4.926-941.2004.
14. **Colombatti M, Johnson VG, Skopicki HA, Fendley B, Lewis MS, Youle RJ.** 1987. Identification and characterization of a monoclonal antibody recognizing a galactose-binding domain of the toxin ricin. J. Immunol. **138:**3339–3344.
15. **McGuinness CR, Mantis NJ.** 2006. Characterization of a novel high-affinity monoclonal immunoglobulin G antibody against the ricin B subunit. Infect. Immun. **74:**3463–3470. http://dx.doi.org/10.1128/IAI.00324-06.
16. **Prigent J, Panigai L, Lamourette P, Sauvaire D, Devilliers K, Plaisance M, Volland H, Créminon C, Simon S.** 2011. Neutralising antibodies

against ricin toxin. PLoS One **6:**e20166. http://dx.doi.org/10.1371/journal.pone.0020166.
17. **Vance DJ, Tremblay JM, Mantis NJ, Shoemaker CB.** 2013. Stepwise engineering of heterodimeric single domain camelid VHH antibodies that passively protect mice from ricin toxin. J. Biol. Chem. **288:**36538–36547. http://dx.doi.org/10.1074/jbc.M113.519207.
18. **Yermakova A, Mantis NJ.** 2011. Protective immunity to ricin toxin conferred by antibodies against the toxin's binding subunit (RTB). Vaccine **29:**7925–7935. http://dx.doi.org/10.1016/j.vaccine.2011.08.075.
19. **Yermakova A, Mantis NJ.** 2013. Neutralizing activity and protective immunity to ricin toxin conferred by B subunit (RTB)-specific Fab fragments. Toxicon **72:**29–34. http://dx.doi.org/10.1016/j.toxicon.2013.04.005.
20. **Yermakova A, Vance DJ, Mantis NJ.** 2012. Sub-domains of ricin's B subunit as targets of toxin neutralizing and non-neutralizing monoclonal antibodies. PLoS One **7:**e44317. http://dx.doi.org/10.1371/journal.pone.0044317.
21. **Lemley PV, Amanatides P, Wright DC.** 1994. Identification and characterization of a monoclonal antibody that neutralizes ricin toxicity in vitro and in vivo. Hybridoma **13:**417–421. http://dx.doi.org/10.1089/hyb.1994.13.417.
22. **O'Hara JM, Neal LM, McCarthy EA, Kasten-Jolly JA, Brey RN, III, Mantis NJ.** 2010. Folding domains within the ricin toxin A subunit as targets of protective antibodies. Vaccine **28:**7035–7046. http://dx.doi.org/10.1016/j.vaccine.2010.08.020.
23. **O'Hara JM, Mantis NJ.** 2013. Neutralizing monoclonal antibodies against ricin's enzymatic subunit interfere with protein disulfide isomerase-mediated reduction of ricin holotoxin in vitro. J. Immunol. Methods **395:**71–78. http://dx.doi.org/10.1016/j.jim.2013.06.004.
24. **Huotari J, Helenius A.** 2011. Endosome maturation. EMBO J. **30:**3481–3500. http://dx.doi.org/10.1038/emboj.2011.286.
25. **Rapak A, Falnes PO, Olsnes S.** 1997. Retrograde transport of mutant ricin to the endoplasmic reticulum with subsequent translocation to cytosol. Proc. Natl. Acad. Sci. U. S. A. **94:**3783–3788. http://dx.doi.org/10.1073/pnas.94.8.3783.
26. **Slominska-Wojewodzka M, Gregers TF, Wälchli S, Sandvig K.** 2006. EDEM is involved in retrotranslocation of ricin from the endoplasmic reticulum to the cytosol. Mol. Biol. Cell **17:**1664–1675. http://dx.doi.org/10.1091/mbc.E05-10-0961.
27. **McEwan WA, Tam JC, Watkinson RE, Bidgood SR, Mallery DL, James LC.** 2013. Intracellular antibody-bound pathogens stimulate immune signaling via the Fc receptor TRIM21. Nat. Immunol. **14:**327–336. http://dx.doi.org/10.1038/nrm3594.
28. **Montfort W, Villafranca JE, Monzingo AF, Ernst SR, Katzin B, Rutenber E, Xuong NH, Hamlin R, Robertus JD.** 1987. The three-dimensional structure of ricin at 2.8 A. J. Biol. Chem. **262:**5398–5403.
29. **Swimmer C, Lehar SM, McCafferty J, Chiswell DJ, Blättler WA, Guild BC.** 1992. Phage display of ricin B chain and its single binding domains: system for screening galactose-binding mutants. Proc. Natl. Acad. Sci. U. S. A. **89:**3756–3760. http://dx.doi.org/10.1073/pnas.89.9.3756.
30. **Houston LL, Dooley TP.** 1982. Binding of two molecules of 4-methylumbelliferyl galactose or 4-methylumbelliferyl N-acetylgalactosamine to the B chains of ricin and Ricinus communis agglutinin and to purified ricin B chain. J. Biol. Chem. **257:**4147–4151.
31. **Sphyris N, Lord JM, Wales R, Roberts LM.** 1995. Mutational analysis of the Ricinus lectin B-chains. Galactose-binding ability of the 2 gamma subdomain of Ricinus communis agglutinin B-chain. J. Biol. Chem. **270:**20292–20297. http://dx.doi.org/10.1074/jbc.270.35.20292.
32. **Yao J, Nellas RB, Glover MM, Shen T.** 2011. Stability and sugar recognition ability of ricin-like carbohydrate binding domains. Biochemistry **50:**4097–4104. http://dx.doi.org/10.1021/bi102021p.
33. **Zentz C, Frénoy JP, Bourrillon R.** 1978. Binding of galactose and lactose to ricin. Equilibrium studies. Biochim. Biophys. Acta **536:**18–26. http://dx.doi.org/10.1016/0005-2795(78)90047-8.
34. **Kimura Y, Hase S, Kobayashi Y, Kyogoku Y, Ikenaka T, Funatsu G.** 1988. Structures of sugar chains of ricin D. J. Biochem. **103:**944–949.
35. **Newton DL, Wales R, Richardson PT, Walbridge S, Saxena SK, Ackerman EJ, Roberts LM, Lord JM, Youle RJ.** 1992. Cell surface and intracellular functions for ricin galactose binding. J. Biol. Chem. **267:**11917–11922.
36. **Wales R, Richardson PT, Roberts LM, Woodland HR, Lord JM.** 1991. Mutational analysis of the galactose binding ability of recombinant ricin B chain. J. Biol. Chem. **266:**19172–19179.
37. **Zhan J, de Sousa M, Chaddock JA, Roberts LM, Lord JM.** 1997. Restoration of lectin activity to a non-glycosylated ricin B chain mutant by the introduction of a novel N-glycosylation site. FEBS Lett. **407:**271–274. http://dx.doi.org/10.1016/S0014-5793(97)00341-4.
38. **van Deurs B, Tønnessen TI, Petersen OW, Sandvig K, Olsnes S.** 1986. Routing of internalized ricin and ricin conjugates to the Golgi complex. J. Cell Biol. **102:**37–47. http://dx.doi.org/10.1083/jcb.102.1.37.
39. **Tekle C, van Deurs B, Sandvig K, Iversen TG.** 2008. Cellular trafficking of quantum dot-ligand bioconjugates and their induction of changes in normal routing of unconjugated ligands. Nano Lett. **8:**1858–1865. http://dx.doi.org/10.1021/nl0803848.
40. **Huttner WB.** 1988. Tyrosine sulfation and the secretory pathway. Annu. Rev. Physiol. **50:**363–376. http://dx.doi.org/10.1146/annurev.ph.50.030188.002051.
41. **Sandvig K, Torgersen ML, Engedal N, Skotland T, Iversen TG.** 2010. Protein toxins from plants and bacteria: probes for intracellular transport and tools in medicine. FEBS Lett. **584:**2626–2634. http://dx.doi.org/10.1016/j.febslet.2010.04.008.
42. **Stechmann B, Bai SK, Gobbo E, Lopez R, Merer G, Pinchard S, Panigai L, Tenza D, Raposo G, Beaumelle B, Sauvaire D, Gillet D, Johannes L, Barbier J.** 2010. Inhibition of retrograde transport protects mice from lethal ricin challenge. Cell **141:**231–242. http://dx.doi.org/10.1016/j.cell.2010.01.043.
43. **Noel R, Gupta N, Pons V, Goudet A, Garcia-Castillo MD, Michau A, Martinez J, Buisson DA, Johannes L, Gillet D, Barbier J, Cintrat JC.** 2013. N-methyldihydroquinazolinone derivatives of retro-2 with enhanced efficacy against Shiga toxin. J. Med. Chem. **56:**3404–3413. http://dx.doi.org/10.1021/jm4002346.
44. **Krautz-Peterson G, Chapman-Bonofiglio S, Boisvert K, Feng H, Herman IM, Tzipori S, Sheoran AS.** 2008. Intracellular neutralization of Shiga toxin 2 by an A subunit-specific human monoclonal antibody. Infect. Immun. **76:**1931–1939. http://dx.doi.org/10.1128/IAI.01282-07.
45. **Smith MJ, Melton-Celsa AR, Sinclair JF, Carvalho HM, Robinson CM, O'Brien AD.** 2009. Monoclonal antibody 11E10, which neutralizes Shiga toxin type 2 (Stx2), recognizes three regions on the Stx2 A subunit, blocks the enzymatic action of the toxin in vitro, and alters the overall cellular distribution of the toxin. Infect. Immun. **77:**2730–2740. http://dx.doi.org/10.1128/IAI.00005-09.
46. **Song K, Mize RR, Marrero L, Corti M, Kirk JM, Pincus SH.** 2013. Antibody to ricin a chain hinders intracellular routing of toxin and protects cells even after toxin has been internalized. PLoS One **8:**e62417. http://dx.doi.org/10.1371/journal.pone.0062417.
47. **Bolte S, Cordelières FP.** 2006. A guided tour into subcellular colocalization analysis in light microscopy. J. Microsc. **224:**213–232. http://dx.doi.org/10.1111/j.1365-2818.2006.01706.x.
48. **Neal LM, O'Hara J, Brey RN, Mantis NJ, Brey RN, III, Mantis NJ.** 2010. A monoclonal immunoglobulin G antibody directed against an immunodominant linear epitope on the ricin A chain confers systemic and mucosal immunity to ricin. Infect. Immun. **78:**552–561. http://dx.doi.org/10.1128/IAI.00796-09.